Atmospheric Research 132–133 (2013) 423–433

Contents lists available at ScienceDirect

Atmospheric Research

journal homepage: www.elsevier.com/locate/atmos

Some characteristics of lightning activity and radiation source distribution in a squall line over north China

Dongxia Liu [a,*], Xiushu Qie [a], Lunxiang Pan [a], Liang Peng [a,b]

[a] Key Laboratory of Middle Atmosphere and Global Environment Observation (LAGEO), Institute of Atmospheric and Physics, Beijing, 100029, China
[b] National Center of Atmospheric Research, Boulder 80302, USA

ARTICLE INFO

Article history:
Received 22 February 2013
Received in revised form 19 June 2013
Accepted 21 June 2013

Keywords:
Squall line
Lightning radiation sources
Charge structure
SAFIR3000
Doppler radar

ABSTRACT

Using the data from SAFIR3000 lightning detection network and Doppler weather radar, the characteristics of lightning activity in a squall line on July 31, 2007 were analyzed. In this study, the lightning activity and inferred charge structure of squall line were obtained. Our results reveal that: 1) the horizontal projection of the lightning radiation sources mainly corresponded to the high radar reflectivity area of the squall line, and 2) the vertical distribution of the lightning radiation sources developed from two layers into three layers. At the developing stage of squall line, the upper lightning radiation sources were centered at 11 km MSL, while the lower radiation sources were located at 4 km MSL. Assuming that the maximum lightning radiation sources were corresponding to the positive charge region, the squall line showed a dipole charge structure with an upper positive charge region and a lower negative charge region. At its mature stage, the entire squall line was characterized by a multi-layer charge structure with three layers of positive charge at 5 km MSL, 9.5 km MSL, and 13 km MSL, and a two-layer negative charge region at 7 km MSL and 11 km MSL.

1. Introduction

Squall line is usually composed by a series of linearly distributed convective cells. The area influenced by squall line is not only accompanied with gust, cold temperature, but also with high impact weather events such as the frequent lightning activity and heavy precipitation. Therefore, the study of concomitant kinematics, microphysics, electrification, and lightning activity of squall line has received considerable research attention. However, in comparison to the research of lightning activity of the MCS (mesoscale convective system) and super cell, the study of the lightning activity in the squall line is relatively rare.

Lightning information not only indicates the intensity and development of the convection, but also forecasts the storm development. Studies of lightning activities combined with the dynamical or microphysical processes of the thunderstorm will reveal the charge structure of a thunderstorm and provide a theoretical reference for forecasting lightning activities in severe weather (Williams et al., 1989; Feng et al., 2009; Qie et al., 1993).

Mazur and Rust (1983) analyzed the lightning activity in a squall line by the total lightning data, and found that the density of total lightning in the convective line is greater than that in the trailing stratiform region. With the development of the lightning location system in VHF band, such as LDAR (lightning array detection ranging), SAFIR3000, and LMA (lightning mapping array) (Boccippio et al., 2001; Chèze and Sauvageot, 1997; Rison et al., 1999; Krehbiel et al., 2000), the lightning VHF radiation pulses could be positioned in 3-dimensional with high accuracy. Zhang et al. (2004) used

* Corresponding author. Tel.: +86 1082995422.
E-mail address: liudx@mail.iap.ac.cn (D. Liu).

0169-8095
http://dx.doi.org/10.1016/j.atmosres.2013.06.010

LMA VHF radiation sources to examine the charge distribution of two super cells with inverted charge structure. Based on LDARII observations, Carey et al. (2005) found that the convective region of the thunderstorm showed a tripole charge structure with the negative charge region centered roughly at 7 km with a comparative minimum density of the lightning radiation sources and the positive charge region centered at 4.5 km and 9.5 km, respectively. Based on the LDAR network, Ely et al. (2008) and Hodapp et al. (2008) investigated the lightning VHF radiation sources of MCS and obtained a charge structure distribution similar to that of Carey et al. (2005). Dotzek et al. (2005) obtained the lightning activity of the squall line and suggested the presence of a tilted dipole charge structure. At the mature stage, the radar reflectivity with lightning activities demonstrated two major discharge layers in the rearward of the convective leading line edge region, and the upper IC lightning zone dropped into the stratiform region. An accurate lightning network was developed by Zhang et al. (2010) in China, the tripolar charge structure of storm in east China was deduced by seven-station observation. By comprehensive lightning observation, Qie et al. (2005) and Zhang et al. (2009) discussed the possible charge structure of thunderstorm in Tibetan Plateau and demonstrated a tripole charge structure.

Electrical sounding can detect the charge structure of storm directly, however only the charge information along the balloon pathway can be recorded. Marshall et al. (1995) examined the distribution of the charge structure in the squall line, and found that two layers of positive charge region located in the layer, are higher than the level with the temperature of 0 °C. By matching videosonde observation of a squall line with radar data, Takahashi and Keenan (2004) obtained the electrification information of different hydrometeor particles and the distribution of charge structure in the convective region and stratiform region.

There are two methods of detecting charge structure of thunderstorms, direct sounding observation and lightning location network. However, both methods have deficiency in China. Yuan and Qie (2010) investigated the lightning activity and its relationship with the precipitation distribution of a squall line over China using precipitation radar (PR), microwave imagining (TMI), and lightning imaging senor (LIS) onboard the TRMM satellite. The results showed that the lightning mainly occurred in the radar contour between 35 dBZ and 50 dBZ and fewer lightning flashes are located in the storm regions with the reflectivity less than 30 dBZ. Although the total lightning information are obtained by the TRMM satellite, the storm is only observed by the satellite sweeping over fix time and fix area due to the orbit limitation. Liu et al. (2011) analyzed the characteristics of the total lightning activities of a LLTS-MCS by SAFIR3000 lightning detection system, but without much discussion of charge structure.

Aforementioned researches shed new light on the lightning activity of severe storm that the lightning propagation and lightning location are significantly related to the charge structure distribution of thunderstorm. Due to the detection accuracy limitation, it is not easy to get the good lightning information in well-organized thunderstorms. By the lightning radiation observation, a typical squall line with electrical information was investigated. So, the aim of this work is to analyze the lightning activity of a squall line in northern China by the SAFIR3000 lightning detection system and Doppler radar. Meanwhile, we also discuss the characteristic of lightning radiation source distribution and the inferred charge structure of the squall line.

2. Data and methods

The lightning data used in this study were obtained by SAFIR 3000 lightning detection system, composed by 3 sensors with about 120 km distance which covered an area about 270–280 km^2 (as shown in Fig. 1). Zheng et al. (2010) noted that the efficiency of the SAFIR 3000 lightning detection network center reached to 90%, the horizontal location error is 2 km and vertical error is less than 2 km. The antenna array in each sensor measured the phase difference of lightning electromagnetic waves to accomplish long-distance lightning detection. The long-range location of total lightning discharge including CG and IC lightning is acquired by triangulation performed on GPS (global position system) time-synchronized provided by three different interferometric sensors with the direction of arrival method. SAFIR 3000 lightning detection system detected from VHF (very high frequency) with the frequency from 110 to 118 MHz to LF (low frequency) with the frequency from 300 Hz to 3 MHz. Lightning flash characteristics are obtained such as time, polarity location, peak current and error. Two types of IC lightning are confirmed, one is the isolated intracloud events with one single location and the other is composition of several events. Some studies (e.g. Mazur et al., 1997; Zheng et al., 2010) by means of the SAFIR3000 lightning data indicated that the detection system provided application value lightning information and high detection efficiency, accuracy, and reliability. Compared with the LDAR II or LMA (Krehbiel et al., 2000; Goodman et al., 2005), the accuracy of SAFIR 3000 lightning detection network is relatively lower, but it still provided the evolution of the total lightning information which could reveal the characteristics of the lightning activities of thunderstorm.

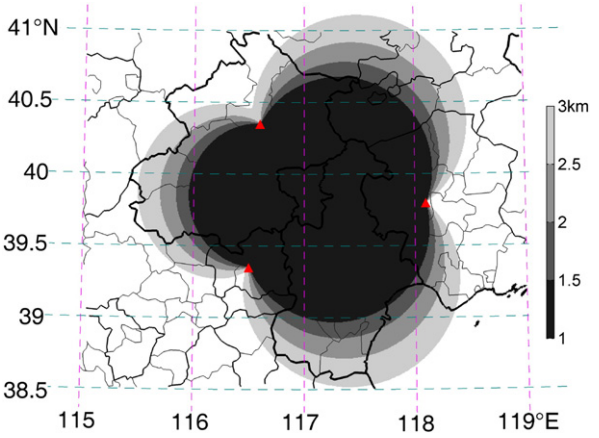

Fig. 1. The distribution of three substations of SAFIR 3000 lightning detection system and the detection efficiency, ▲ stands for the location of the detected substation.

Lightning information from the SAFIR 3000 system was filtered in this work for the accuracy of total lightning data. For determining the lightning number, the lightning with the same polarity occurred in one second and the distance less than 7 km is defined as one flash. Meanwhile, the lightning's position is considered as the location of the first lightning radiation source. The discrimination standard between the IC and CG flashes in the SAFIR 3000 lightning data is the height item information. According to the study of Wang and Liao (2006), the IC flashes seldom occurred in the level lower than 1 km, so here, only the lightning radiation sources with height item higher than 1.0 km are considered. Secondly, based on the research of Cummins et al. (1998), not all the positive discharges with peak current between 5 kA and 15 kA are identified as + CG flashes. Therefore, the current value of 10 kA is regarded as a standard for distinguishing + CG flashes and IC flashes in this study. But for the − CG flashes, the standard is the negative polarity of lightning. It is recommended that weak positive polarity discharges with peak currents being less than 10 kA should be considered as IC discharge.

The radar data are obtained from S-band Doppler radar located at 39.814°N and 116.472°E available from the Beijing Meteorological Administration. It has the 7-level elevation scan every 6 min and covers a range of 230 km radius.

3. The lightning activity of the squall line

3.1. The evolution of total lightning characteristics and radar reflectivity

A squall line originated in the northwest direction and moved passing by the radar site to the southeast on 31th July 2007 and lasted about 8 h starting from 12:30 LST to 18:00 LST (local standard time). From the initial to its disappearance, the storm mainly influenced over Beijing area and its vicinity region in the detection range. The squall line was accompanied by the gust, precipitation and frequent lightning. The entire lifetime of the squall line was separated into developing stage from 12:30 LST to 14:00 LST, mature stage from 14:00 LST to 16:00 LST, and dissipating stage after 16:00 LST.

Fig. 2(a–d) showed the distribution of total lightning including IC lightning and CG lightning combined with radar reflectivity in different times of the developing stage. During this period, the convective region was comprised by several convective cells which originated, developed, and vanished continuously. At 13:18 LST, the squall line was organized by a series of convective cells with a stratiform region in the rearward (Fig. 2a). Convective line was characterized by high

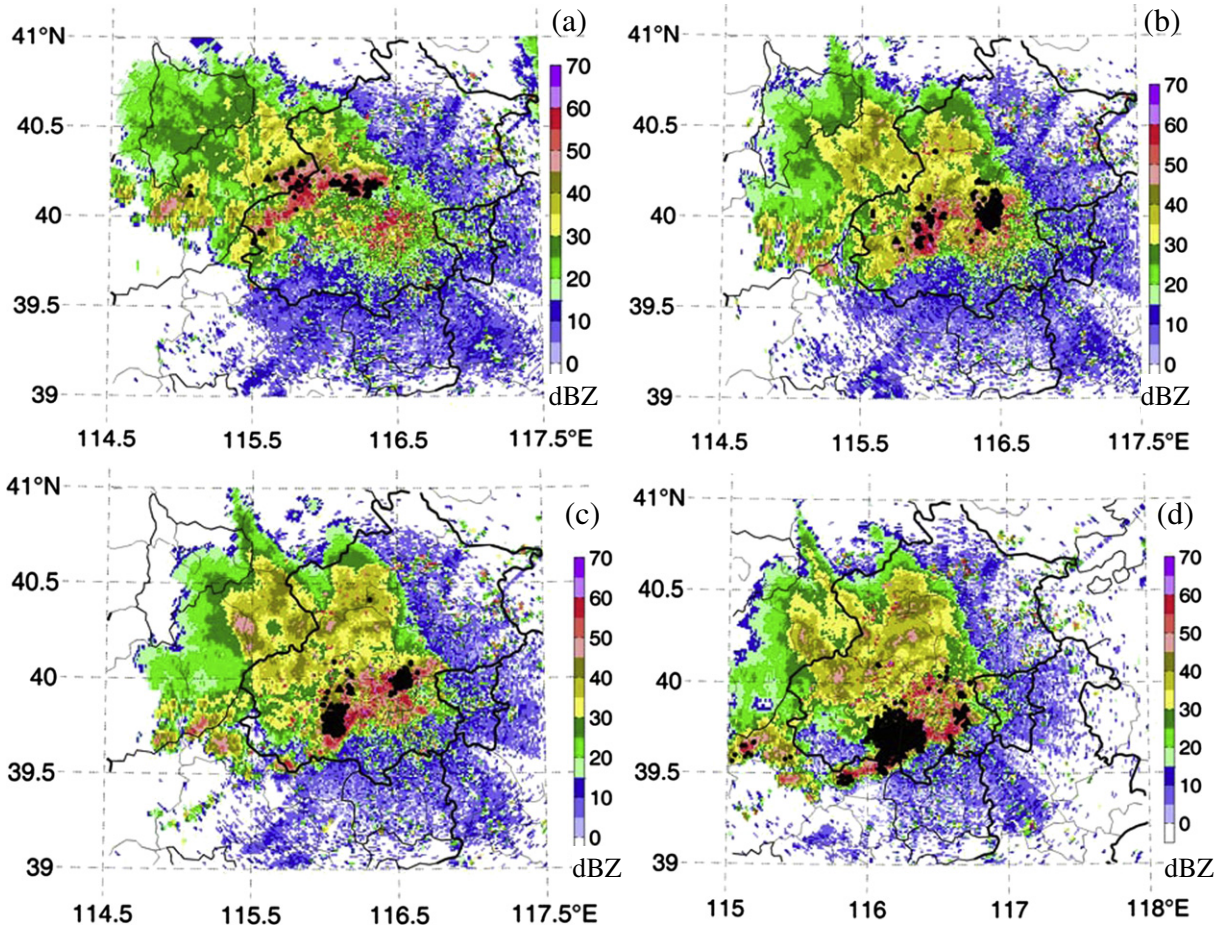

Fig. 2. The lightning location and the compose radar reflectivity within 6 min in four times. Black dot stands for intra-cloud lightning and black triangle stands for cloud-to-ground lightning. (a) 13:18, (b) 13:36, (c) 13:42, (d) 13:54 LST.

value radar reflectivity (45–60 dBZ), the stratiform region was accompanied with 35–40 dBZ. Majority of lightning occurred in the high radar reflectivity of the convective region. At 13:36 LST (Fig. 2b), the convective line was separated into two parts with the reflectivity increased to the maximum of 60 dBZ and the extended speed of stratiform region was faster than the previous period. The lightning mainly occurred around and in the strong radar echo of the squall line, especially the eastern convective cell.

In Fig. 2c, the convective region showed apparently linear distribution and perpendicular to the storm motion. Some maxima reflectivity occurred in the stratiform region. The occurrence frequency of the lightning increased apparently and the lightning formed two centers which mainly concentrated in the convective leading line, while sporadic lightning occurred in the stratiform region with the radar echo greater than 30 dBZ. Comparing the distribution of lightning during this period with that during the previous period, most of the lightning flashes occurred in the western part of the convective region which indicated that the discharge moved from eastern cell to the western one (Fig. 2b–c). As shown in Fig. 2d, at 13:54 LST, a strong radar echo merged together and an apparent hook radar echo appeared in the core of convective region of the squall line which was companied with the gust, while the surface gust reaches to 18 m/s from the ground-based observation. With the number of the lightning increasing, most of the lightning were located in the backward of the convective line. The possible reason was that the charge structure of the squall line showed slightly slant, because the inside airflow from the convective region descended to the stratiform region.

Fig. 3(a–d) depicted the lightning superimposed on the radar image in the mature stage within 6 min. During this period, the squall line was an effective rain producer, and the scale and the intensity of radar reflectivity obviously reached a stationary peak level. The number of lightning apparently increased in this period. At this stage, the storm was accompanied with frequent and abundant IC lightning activities, as recorded by the SAFIR3000 lightning detection system and ground-based optics instrument over this area. At 14:18 LST the bow echo appeared in the convective region and the strong downdraft started in front of the leading line of the squall line. Radar reflectivity reached to maxima of 65 dBZ in convective line and 50 dBz in the stratiform region. During this period, the storm strengthened quickly and the CG lightning increased, although the IC lightning still predominated. The lightning was concentrated significantly in the high radar

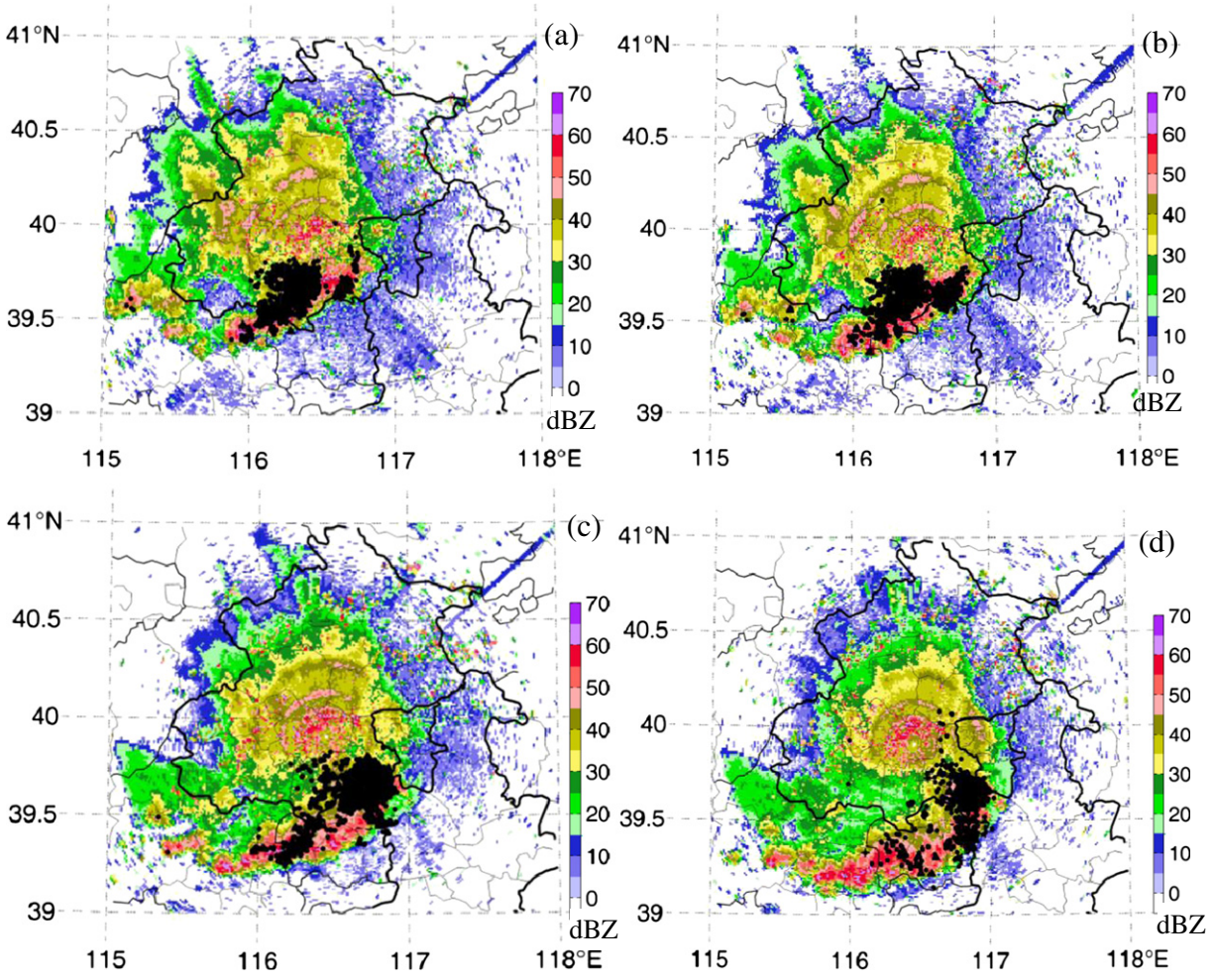

Fig. 3. Same as Fig. 2 but at mature stage. (a) 14:18, (b) 14:24, (c) 14:36, (d) 14:54.

reflectivity which was greater than 40 dBZ, and there were only two lightning flashes that occurred in the stratiform region. There appeared a high density center of lightning distribution along the convective leading line in the southwest of the squall line. As shown in Fig. 3b, at 14:24 LST, the storm moved slower than at the developing stage. The trail of the leading line bent to backward, and a bright band of radar echo appeared in the stratiform region. It was noticed that new isolated convective cells were generated in the back of trailing line which indicated a prolonged curve combined with convective line. The amount of lightning was larger than that in the last period, the CG lightning apparently increased and located in the convective leading region, especially, the bulk of the lightning located in the southwest of the system. During the period of 14:36–14:54 LST (Fig. 3c and d), the intensity and the scale of the convective leading line region reached to their maximum. New isolated cells intensified gradually and closed up to the leading region. Finally, the cumulonimbus cells merged into the convective leading line (Fig. 3d). The lightning was clustered in a northeast sector of the squall line where the radar contour of convective leading edge decreased sharply, and sporadically dispersed in the stratiform region. In the period of 15:00 LST, there existed a clear bow radar echo in the area with high radar reflectivity of the thunderstorm.

With the thunderstorm developing into its dissipating stage (Fig. 4a), the high radar reflectivity area formed into obvious bowed convective region and decreased stratiform region. The lightning activity went into quiet-period and the number of lightning decreased obviously. At 16:18 LST, the distribution of convective line was still clear, developing to 16:42 LST, a strong radar echo started to break into pieces and the number of the total lightning diminished significantly. As seen in Fig. 4d, the convective region only remained by weak radar reflectivity and the whole convective line disappeared. The lightning located in the stratiform region increased apparently in the dissipating stage, as compared to that in the mature stage. Carey et al. (2005) provided a hypothesis that the hydrometeor particle presented active under the strong updraft in the convective region, the collision rate and transfer processes between the hydrometer particles both increased. The updraft reached to the top of the thunderstorm and declined to the stratiform region, and the charge particles moved from the convective region to the stratiform region by the airflow. The increase of stratiform region lightning was caused by the electrification

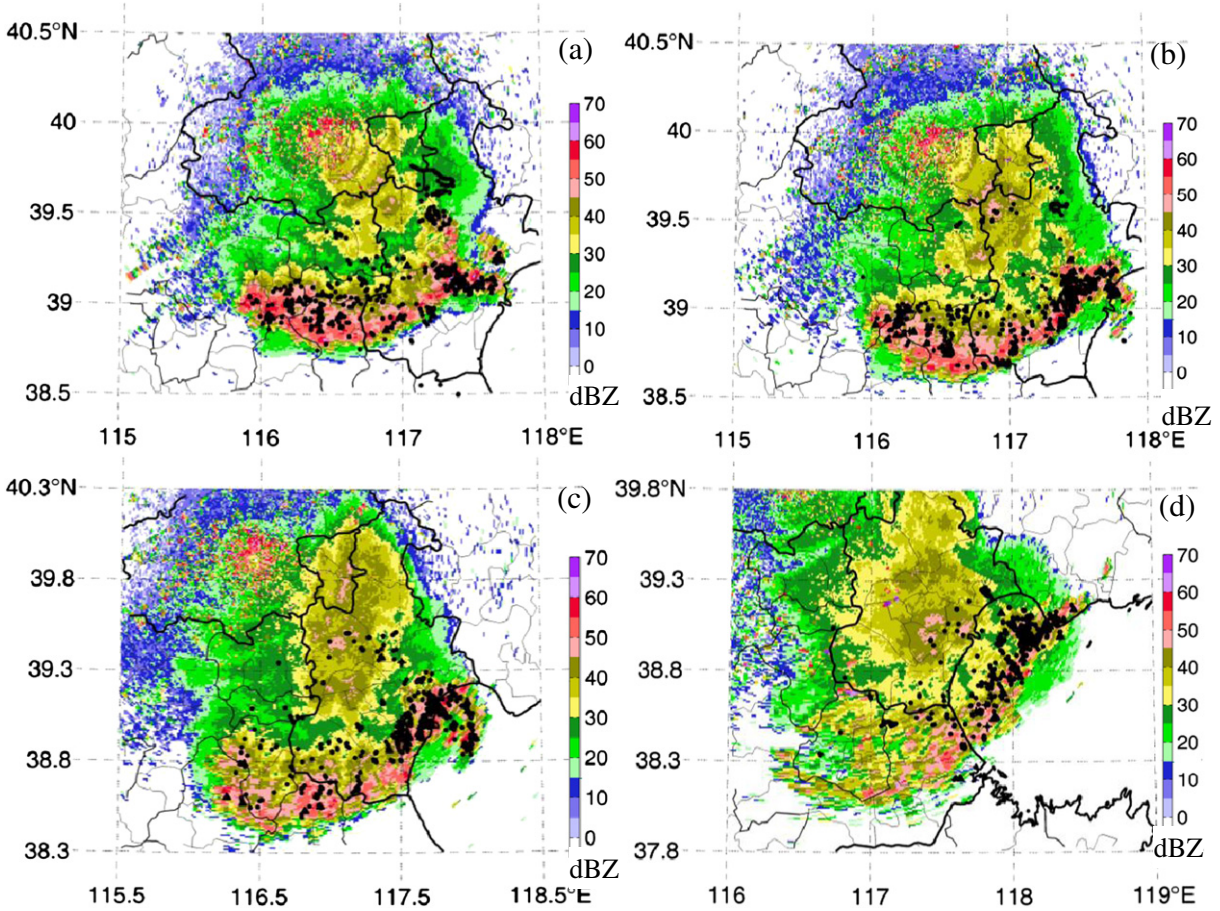

Fig. 4. Same as Fig. 2 but at the dissipating stage. (a) 15:48, (b) 16:18, (c) 16:42, (d) 17:36.

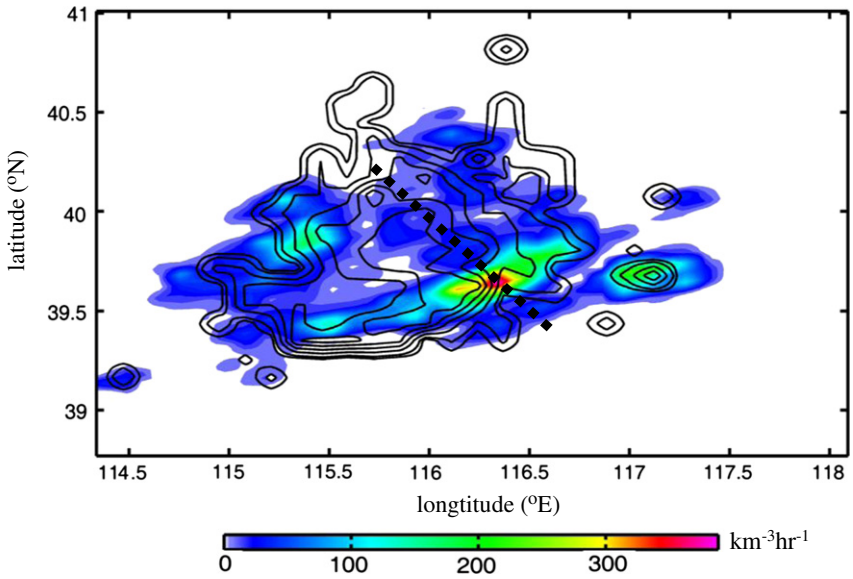

Fig. 5. The distribution of the lightning radiation and radar echo within 30 min at 14:24. The black solid line is the radar echo from 10 dBZ to 60 dBZ with an interval of 10 dBZ, the dash line is the cross-section from convective region to stratiform region along the strongest lighting radiation \ within the range of 0.1° in the tangent line.

itself and the charge particles were transported from the convective region.

3.2. The distribution of lightning radiation sources

Because the storm developed and disappeared within the range of lightning detection network system with the detection efficiency up to 90%, the majority of lightning were detected. In order to understand the relationship of lightning distribution and the charge structure of the squall line, horizontal lightning radiation sources were imposed on radar echo image. Fig. 5 showed lightning radiation sources occurring in 30 min coupled with the radar image at 14:24 LST in the mature stage. There was a good correlation between the lightning radiation distribution and radar echo during the period of 14:00–14:30 LST. The distribution of lightning radiation sources corresponding to the radar contour demonstrated that the lightning radiation sources with high value distributed in strong radar echo and gradually decreased to the stratiform region. This implies that the electrification mechanism might take place in this region, in accordance with the findings of Dotzek et al. (2001) and Carey et al. (2005). Within the convective region, a layer of dominated electrical active lightning radiation sources distributed apparently along the convective leading line from the northeast to southwest direction of the storm. The secondary center of lightning radiation sources appeared in the stratiform region, and were apparently smaller than the center in the convective leading line. The highest value of the lightning radiation sources, which appeared in the convective region was approximately ten times larger than that in the stratiform region. In other periods of the squall line, the distribution of lightning radiation sources with radar contour exhibited the same feature (not shown here). The lightning radiation source distribution in the stratiform region was classified into two categories: (1) a charge transfer mechanism, and (2) a electrification mechanism. Beside the charging electrification mechanism in the stratiform region, parts of the radiation VHF sources were transported from the convective region. Carey et al.(2005) explained the phenomenon that the lightning pathway was transported downward and rearward from the high level of the convective line to the stratiform region. It is similar to the way of snow particles transferred from the convective line by the airflow. Because of their remarkable larger fall speed, they descended downward to the melting level by the weak updraft, then formed the radar bright band.

Fig. 6(a–b) showed the lightning radiation sources evoluting with the altitude at three different periods of the squall line, which was along the tangent lines across the density center of radiation sources within 0.1° from the convective region to the stratiform region, and accompanied with radar contour. Fig. 6a documented the distribution of lightning radiation sources during the period of 13:30–13:59 LST, which mainly occurred in the level of 2–12 km and dispersed in the lower level without obvious high value. There was a peak value area in the level of 10 km, which indicated that the frequent discharge occurred in this level. It is noticed that the peak value of lightning radiation sources does not just correspond to the high reflectivity region but appreciably behind it. Convective cells developed and dissipated continuously, hence the center of the lightning radiation sources was followed by the new cell generation leading to the lightning clustered in different zones of the convective line that are manifested apparently in Fig. 2c. MacGorman et al. (2001) pointed out that the discharge usually occurred between the two-layer charge region then propagated into the charge layers upward and downward, respectively. The lightning radiation sources generated by the negative streamer is usually stronger than those by the positive streamer. The negative leader is easy to detect when propagating in the positive charge region. By contrast, the leader of positive is rarely detected. As reviewed by Carey et al. (2005), we assumed that maximum of lightning radiation source density is reasonably

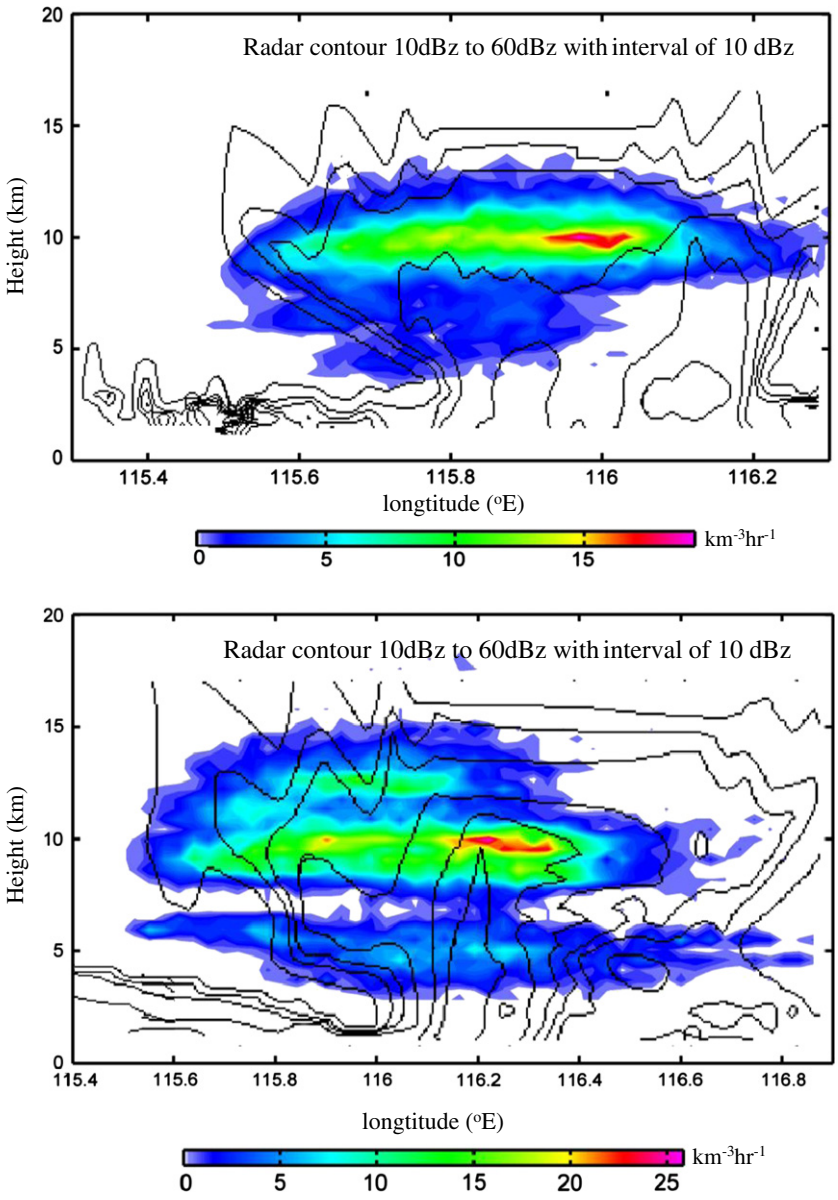

Fig. 6. The evolution of the density of lightning radiation source changed with the height within 30 min in the squall line. The range of lightning radiation is the cross-section showed within 0.1°. Radar contour distributed from 10 dBz to 60 dBz with an interval of 10 dBz.

associated with positive charge region. That is, the center of lightning radiation sources was corresponding to the negative streamer spreading into the positive charge region, and the minimum of lightning radiation sources was considered as the positive streamer propagating into the negative charge region. So it was implied by Fig. 6a that during the period of 13:30–13:59 LST, the squall line presented a dipole charge structure with the negative charge region in the lower level and the positive charge region in the upper high level. The forming of the stable charge region mainly depended on the hydrometeor particles colliding with each other which lead to the charge separation by the updraft at the moment during the developing stage came into the mature stage.

With the squall line developed into its mature stage, the center of lightning radiation sources was just above the area of the highest radar reflectivity, corresponding to the updraft zone with severe electrification and frequent lightning discharge. The lightning radiation sources and the whole charge structure were both elevated to higher level. The lightning radiation sources in the high level were formed by the negative streamer propagating in the positive charge layer which was relatively weak located at the 13 km during the period of 14:00–14:29 LST. At the middle level of the 9.5 km, the peak value of the lightning radiation sources reached to 27 km^{-3} h^{-1}. There was a charge junction area which appeared in the level of 7 km between the upper radiation source layer and the middle layer. Another lower

weak lightning radiation source area generated from the level of 3 km to 7 km above the melting layer with the temperature from 0 to −25 °C and the unclear center located at the level of 5 km in height.

At the level of 9.5 km, the lightning radiation sources predominated indicating that the positive charge region occupied a large range, and the other two maxima (near 5 km and 13 km) were also logically associated with positive charge. Meanwhile, the negative charge resided between these regions with less lightning radiation source density, forming a complex multipolar charge structure. We speculated that during this period, the charge structure of squall line presented five layers with a major positive charge region centered at the level of 9.5 km, additional positive charge region centered at the level of 5 km and 13 km, and negative charge region centered at 7 km and 11 km with the relative minimum of the radiation source density. Compared with the previous period, the charge region elevated about 2 km in the convective region. With the squall line being developed, the discharge layer was elevated by the strong updraft, leading to the lightning radiation sources being lifted to a higher level.

Overall, the squall line exhibited a two-layer charge structure that can be characterized by negative charge in the lower level and positive charge region in the upper level in the early stage. With the squall line being developed, the other area of lightning radiation sources appeared beneath and above the major discharge region. The squall line exhibited a multi-layer charge structure.

3.3. Discussion of the charge structure

Fig. 7 showed the CG lightning imposed on the radar image at 14:42 LST in the mature stage. It was noticed that +CG lightning predominated in this period with high percentage in the convective region compared with the −CG lightning. Both of the +CG and −CG flashes distributed densely in the northeastern of the squall line where the frequent lightning discharge appeared here. Usually there are usually two major charge layers forming in the thunderstorms, including a positive charge region higher, near the level with a temperature of −40 °C and a negative charge layer between the temperature of −10 °C to −20 °C. Beside the main dipole charge structure distribution, weak charge layers might exist in the thunderstorm, for example, a smaller positive charge layer usually came forth in the bottom of the storm near the freezing level, resulting in a tripole charge structure distribution. But for the +CG lightning, there existed different known processes.

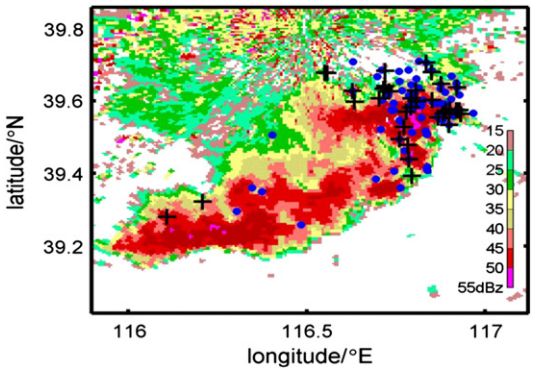

Fig. 7. The +CG and −CG lightning location superimposed with the compose radar reflectivity within 5 min at 14:42 LST. "+" stands for the +CG lightning, blue dots stand for the −CG lightning.

Williams (2001) listed several hypotheses about +CG flashes dominated in storm i.e., the tripole charge structure, the inverted dipole, and the tilted dipole. The lower positive charge of the tripole charge structure strengthened and played an important role in producing ground flashes. Inverted dipole is opposite with the common charge structure of the positive charge in the lower level near the ground and the negative charge in the upper level, hence the positive charge region is more easy to discharge (Rust et al., 2005). The tilted dipole structure is caused by the lateral displacement of upper positive charge, which related to the main negative charge because of the upper airflow and the sloping updraft. By this way, the positive charge region could not be shielded overhead from the ground by the negative charge region layer anymore, leading to the occurrence of +CG lightning. Considering the lightning radiation source distribution, the whole squall line showed a multi-layer charge structure pattern, with the upper positive charge region occupying overhead the negative region causing the +CG lightning dominated in a certain period. Therefore, −CG lightning predominated in the whole squall line and +CG lightning dominated in developing-mature period caused by larger positive-charge structure.

Combining the characteristics of lightning radiation sources with the lightning activities, the charge structure conceptual model of squall line was deduced. At the developing stage, the squall line indicated the dipole charge structure with lower negative charge and the upper positive charge. With the squall line developing and the charge region uplifting into the upper layer, the electrical ice phase particles aggregated formed a stable positive charge region. When the system came into the mature stage, the squall line demonstrated a multi-layer charge structure. At the dissipating stage, the intensity and scale of the lightning radiation sources both decreased, leading to weak charge distribution. Furthermore, the charge intensity was decreased gradually by the weak electrification. Stolzenburg et al. (1998) found that the main charge region usually exist with a weak shield charge layer which is located in the top of storm. There might exist an additional charge layer in the top of the thunderstorm. More observations are necessary for further study on this issue.

4. Lightning frequency of the squall line

Fig. 8(a–b) showed the evolution of total lightning and CG lightning frequencies. During the whole lifetime of squall line, the lightning increased at the beginning and then decreased gradually (Fig. 8a). At the mature stage, IC lightning and CG lightning both reached their peak values and the lightning frequency was up to 1320 flashes/5 min. With the squall line into its dissipating stage, the lightning frequency decreased gradually.

Although the −CG lightning almost predominated in the entire lifetime of the squall line, the amount of the +CG lightning was larger than the −CG lightning in a certain period of the mature stage (13:50 LST–14:50 LST). To some

extent, the results confirmed the charge structure with a large positive charge region.

5. Conclusions and discussions

The lightning activities and the radiation source distribution of the squall line were analyzed in this study. The squall line moved fast with the convective leading line forward and stratiform region backward. The horizontal range of the storm was about 200 km and the vertical distribution of the lightning radiation sources reached to 16 km.

Most of the lightning radiation sources were located in the strong radar echo, especially in the convective core of squall line. When the squall line developed into the dissipating stage, the occurrence frequency of lightning in the stratiform region gradually increased.

For the spatial distribution of lightning radiation sources, most were located in the convective leading line and gradually declined into the stratiform region. The squall line presented a two-layer discharge with lightning radiation sources concentrated at the level of 11 km upward and sporadically located at 4 km downward. Charge structure of the squall line was inferred as a dipole charge structure with the upper positive charge and the lower negative charge region in the developing stage, and multi-layer charge structure with five layers in the mature stage, as proved by the lightning radiation source distribution. Carey et al. (2005) analyzed the lightning radiation sources in a MCS, the upper discharge layer centered

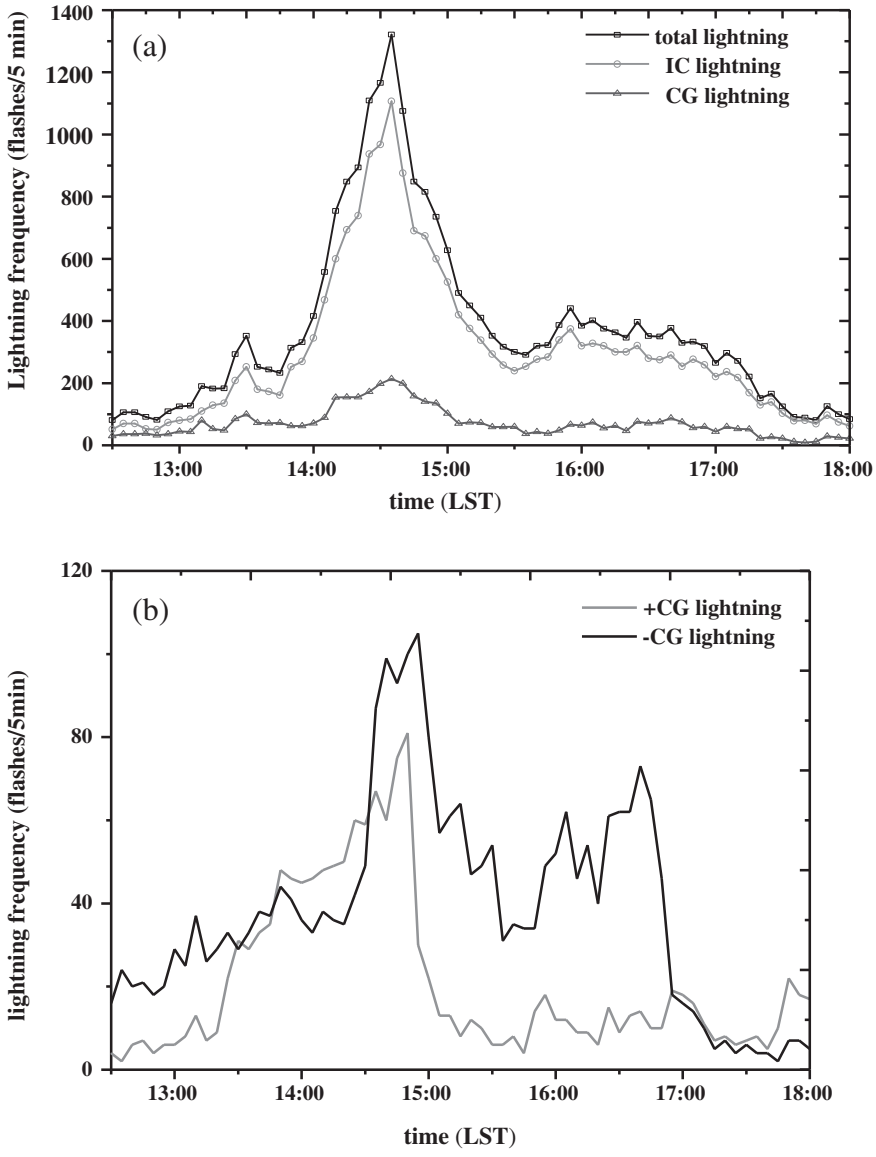

Fig. 8. Evolution of the total lightning frequency (a) and CG lightning frequency (b) within 5 min.

at the level of 10 km and the lower discharge centered at the level of 4 km. The thunderstorm indicated the tripolar charge structure with positive charge centered at 4.5 km and 9.5 km and negative charge centered at 7 km. Although the charge structure is inconsistent with the result of our work, the discriminated approach of charge region by lightning radiation source distribution is similar. Over Tibetan Plateau, storms demonstrated tripole charge structure with large bottom positive charge region (Qie et al., 2005), but showed normal tripolar type over inland region in north plain of China (Zhang et al., 2010). Other observational results showed that the thunderstorm presented different categories with dipole pattern (Williams, 2001), inverted charge structure (Rust et al., 2005) or multi-layers (Stolzenburg et al., 1998) which is in agreement with our results of the squall line. Considering the complex electrification and lightning propagation in thunderstorm and the regional difference, the charge structures of storms are different.

Under the electrification and discharge processes of the thunderstorm, charge structure is formed by the interaction between dynamical and microphysical processes. Different charging mechanisms could influence the electrification condition and then formed different types of charge structure. Mansell et al. (2005) compared five non-inductive parameterizations and found that three of them demonstrated tripole charge structure and two of them showed dipole charge structure. This explained the simulation of the electrification depending on the different parameterizations. Under the non-inductive parameterization, the charge transfer rate of graupel–ice crystals in the positive region is larger than that in the negative charge region. The content of graupel is required to be large enough in order to form larger positive charge, while the graupel producing the negative charge should not be too big to decrease the positive charge density as well. Because of the large scale of positive charge region, +CG lightning predominated during a certain period.

Due to the limitation of detection capability, it is difficult to decide how the dynamical, microphysics and electrification processes influence the charge structure distribution of the squall line. Future works will combine the model simulation with sounding observation to deepen our understandings on the lightning activity of the squall line based on more cases.

Acknowledgments

This work was supported by the National Natural Science Foundation of China (Grant Nos. 40930949, 41105002), and supported by the Strategic Priority Research Program on Space Science, the Chinese Academy of Sciences (Grant No. XDA04072400). The authors thank Beijing Meteorological Administration for providing the lightning detection data and radar data.

References

Boccippio, D.J., Heckman, S., Goodman, S.J., 2001. A diagnostic analysis of the Kennedy Space Center LDAR network 1. Data characteristics. J. Geophys. Res. 106 (D5), 4769–4786.

Carey, L.D., Murphy, M.J., McCormick, T.L., Nicholas, W.S., 2005. Lightning location relative to storm structure in a leading-line, trailing-stratiform mesoscale convective system. J. Geophys. Res. 110, D03105. http://dx.doi.org/10.1029/2003JD004371.

Chèze, J.L., Sauvageot, H., 1997. Area-average rainfall and lightning activity. J. Geophys. Res. 102 (D2), 1707–1715.

Cummins, K.L., Murphy, M.J., Bardo, E.A., Hiscox, W.L., Pyle, R.B., Pifer, A.E., 1998. A combined TOAA/MDF technology upgrade of the U.S. National Lightning Detection Network. J. Geophys. Res. 103, 9035–9044.

Dotzek, N., Holler, H., Thery, C., Fehr, T., 2001. Lightning evolution related to radar-derived microphysics in the 21 July 1998 EULINOX supercell storm. Atmos. Res. 56, 335–354.

Dotzek, N., Rabin, R.M., Carey, L.D., MacGorman, D.G., McCormick, T.L., Demetriades, N.W., Murphy, M.J., Holle, R.L., 2005. Lightning activity related to satellite and radar observation of mesoscale convective system over Texas on 7–8 April 2002. Atmos. Res. 76, 127–166.

Ely, B.L., Orville, R.E., Carey, L.D., Hodapp, C.L., 2008. Evolution of the total lightning structure in a leading line, trailing-stratiform mesoscale convective system over Houston, Texas. J. Geophys. Res. 113, D08114. http://dx.doi.org/10.1029/2007JD008445.

Feng, G.L., Qie, X.S., Wang, J., Gong, D.L., 2009. Lightning and Doppler radar observations of a squall line system. Atmos. Res. 91 (2–4), 466–478.

Goodman, S.J., Blakeslee, R., Christian, H., Koshak, W., Bailey, J., Hall, J., McCaul, E., Buechler, D., Darden, C., Burks, J., Bradshaw, T., Gatlin, P., 2005. The North Alabama lightning mapping array: recent severe storm observations and future prospects. Atmos. Res. 76, 423–437.

Hodapp, C.L., Carey, L.D., Orville, R.E., 2008. Evolution of radar reflectivity and total lightning characteristics of the 21 April 2006 mesoscale convective system over Texas. Atmos. Res. 89, 113–137.

Krehbiel, P.R., Thomas, R.J., Rison, W., Hamlin, T., Harlin, J., Davis, M., 2000. Lightning mapping observations in central Oklahoma. Eos 81, 21–25.

Liu, D.X., Qie, X.S., Xiong, Y.J., Feng, G.L., 2011. Evolution of the total lightning structure in a leading-line, trailing stratiform mesoscale convective system over Beijing. Adv. Atmos. Sci. 28 (4), 1–13.

MacGorman, D.R., Straka, J.M., Ziegler, C.L., 2001. A lightning parameterization for numerical cloud models. J. Appl. Meteorol. 40 (3), 459–478.

Mansell, E.R., MacGorman, D.R., Ziegler, C.L., Straka, J., 2005. Charge structure and lightning sensitivity in a simulated multicell thunderstorm. J. Geophys. Res. 110 (D12) (ACL2-1-2-14).

Marshall, T.C., Rust, D.W., Stolzenburg, M., 1995. Electrical structure and updraft speeds in thunderstorms over the southern Great Plain. J. Geophys. Res. 100, 1000–1015.

Mazur, V.E., Rust, W.D., 1983. Lightning propagation and flash density in squall lines as determined with radar. J. Geophys. Res. 88, 1459–1502.

Mazur, V., Williams, E., Boldi, R., Maier, L., Proctor, D.E., 1997. Initial comparison of lightning mapping with operational time-of-arrival and interferometric systems. J. Geophys. Res. 102 (D10), 11071–11085.

Qie, X.S., Guo, C.M., Yan, M.H., Zhang, G.S., 1993. Lightning data and study of thunderstorm nowcasting. Acta Meteorol. Sin. 7 (2), 244–256.

Qie, X.S., Kong, X.Z., Zhang, G., Yuan, T., Zhou, Y., Zhang, Y., Wang, H., Sun, A., 2005. The possible charge structure of thunderstorm and lightning discharges in northeastern verge of Qinghai–Tibetan Plateau. Atmos. Res. 76, 231–246.

Rison, W., Thomas, R.J., Krehbiel, P.R., 1999. A GPS-based three-dimensional lightning mapping system: initial observations in central New Mexico. Geophys. Res. Lett. 26, 3573–3576.

Rust, W.D., MacGorman, D.R., Bruning, E.C., Weiss, S.A., Krehbiel, P.R., Thomas, R.J., Rison, W., Hamlin, T., Harlin, J., 2005. Inverted-polarity electrical structures in thunderstorms in the Severe Thunderstorm Electrification and Precipitation Study (STEPS). Atmos. Res. 76, 247–271.

Stolzenburg, M., Rust, W.D., Marshall, T.C., 1998. Electrical structure in thunderstorm convective regions.1. Mesoscales convective systems. J. Geophys. Res. 103, 14059–14078.

Takahashi, T., Keenan, T.D., 2004. Hydrometeor mass, number, and space charge distribution in a “Hector” squall line. J. Geophys. Res. 109, D16208. http://dx.doi.org/10.1029/2004JD004667.

Wang, K.Y., Liao, S.A., 2006. Lightning, radar reflectivity, infrared brightness temperature, and surface rainfall during the 2–4 July 2004 severe convective system over Taiwan area. J. Geophys. Res. 111, D05206. http://dx.doi.org/10.1029/2005JD006411.

Williams, E.R., 2001. The electrification of severe storms. In: Doswell, Charles A. (Ed.), Severe Convective Storm. Meteor. Monogr., No.50. Amer. Meteor. Soc, pp. 527–561 (Chapter 13).

Williams, E.R., Weber, M.E., Orville, R.E., 1989. The relationship between lightning type and convective state of thunder clouds. J. Geophys. Res. 94, 13213–13220.

Yuan, T., Qie, X.S., 2010. TRMM-based study of lightning activity and its relationship with precipitation structure of a squall line in South China. Chin. J. Atmos. Sci. 34 (1), 58–70 (in Chinese).

Zhang, Y.J., Meng, Q., Krehbiel, P.R., Liu, X.S., Zhou, X.J., 2004. Spatial and temporal characteristics of VHF radiation source produced by lightning in supercell thunderstorms. Chin. Sci. Bull. 49 (6), 624–631.

Zhang, T.L., Qie, X.S., Yuan, T., Zhang, G.S., Zhang, T., Zhao, Y., 2009. Charge source of cloud-to-ground lightning and charge structure of a typical thunderstorm in the Chinese Inland Plateau. Atmos. Res. 92, 475–480.
Zhang, G.S., Wang, Y.H., Qie, X.S., Zhang, T.L., Zhao, Y.X., Li, Y.J., Cao, D.J., 2010. Using lightning locating system based on time-of-arrival technique to study three-dimensional lightning discharge processes. Sci. China Earth Sci. 53, 591–602. http://dx.doi.org/10.1007/s11430-009-0116-x.
Zheng, D., Zhang, Y.J., Meng, Q., Lu, W.T., Zhong, M., 2010. Lightning activity and electrical structure in a thunderstorm that continued for more than 24 h. Atmos. Res. 97, 241–256.